



Glacial–interglacial variability in Atlantic meridional overturning circulation and thermocline adjustments in the tropical North Atlantic

Raquel A. Lopes dos Santos^{a,*}, Matthias Prange^b, Isla S. Castañeda^a, Enno Schefuß^b, Stefan Mulitza^b, Michael Schulz^b, Eva M. Niedermeyer^{b,1}, Jaap S. Sinninghe Damsté^a, Stefan Schouten^a

^a Royal Netherlands Institute for Sea Research (NIOZ), Department of Marine Organic Biogeochemistry, P.O. Box 59 AB Den Burg, Texel, The Netherlands

^b MARUM—Center for Marine Environmental Sciences, University of Bremen, Leobener Strasse, D-28359 Bremen, Germany

ARTICLE INFO

Article history:

Received 13 August 2010

Received in revised form 15 October 2010

Accepted 20 October 2010

Editor: M.L. Delaney

Keywords:

U_{37}^K

TEX₈₆

Atlantic meridional overturning circulation
thermocline

ABSTRACT

Changes in the strength of Atlantic meridional overturning circulation (AMOC) are known to have profound impacts on global climate. Coupled modelling studies have suggested that, on annual to multi-decadal time scales, a slowdown of AMOC causes a deepening of the thermocline in the tropical Atlantic. However, this process has been poorly constrained by sedimentary geochemical records. Here, we reconstruct surface (U_{37}^K Index) and thermocline (TEX₈₆) water temperatures from the Guinea Plateau Margin (Eastern tropical Atlantic) over the last two glacial–interglacial cycles (~192 kyr). These paleotemperature records show that periods of reduced AMOC, as indicated by the $\delta^{13}C$ benthic foraminiferal record from the same core, coincide with a reduction in the near-surface vertical temperature gradient, demonstrating for the first time that AMOC-induced tropical Atlantic thermocline adjustment exists on longer, millennial time scales. Modelling results support the interpretation of the geochemical records and show that thermocline adjustment is particularly pronounced in the eastern tropical Atlantic. Thus, variations in AMOC strength appear to be an important driver of the thermocline structure in the tropical Atlantic from annual to multi-millennial time scales.

© 2010 Elsevier B.V. All rights reserved.

1. Introduction

The ocean is a fundamental component of the Earth's climate due to its capacity to store and transport large amounts of heat. The Atlantic meridional overturning circulation (AMOC) transports heat through warm (and saline) surface currents from the tropics to the polar and subpolar North Atlantic where heat is released to the atmosphere producing a southward current of cold water in the deep Atlantic (Ganachaud and Wunsch, 2003). It is widely accepted that past variations in AMOC induced substantial changes in the global temperature distribution, wind fields and the hydrologic cycle (Rahmstorf, 2002). Additionally, some climate models predict a slowdown of the AMOC for increased future atmospheric CO₂ concentrations (Gregory et al., 2005). Therefore, it is crucial to gain deeper insight into past AMOC variations and their impact on ocean properties.

Previous studies, using coupled climate models and observational data, showed that an anticorrelated variation between surface and subsurface temperature in the tropical North Atlantic is a distinctive signature of AMOC variability on (multi-)decadal time scales (Chiang

et al., 2008; Zhang, 2007) that is clearly distinguishable from the response pattern of external radiative forcing (Zhang, 2007). The physics behind these temperature variations have been investigated in previous studies: upon AMOC slowdown, strengthened northeast trade winds, associated with a southward displacement of the Atlantic intertropical convergence zone, tend to cool the surface of the tropical North Atlantic mainly due to enhanced evaporative latent heat fluxes (Chiang et al., 2008; Zhang, 2007), a process that cannot be simulated with uncoupled ocean-only models. Simultaneously, subsurface waters in the tropical Atlantic warm due to reduced import of relatively cold water into the tropical Atlantic from the south and reduced warm-water export to the north (Chiang et al., 2008). This goes along with a deepening of the permanent (Huang et al., 2000; Rahmstorf, 2002) and tropical (Haarsma et al., 2008) thermoclines, accomplished by rapid baroclinic wave adjustment processes (Zhang, 2007).

Although this process is well documented on (multi-)decadal time scales, it is not known how important this pattern of tropical upper-ocean temperature is on longer, millennial time scales, both from a modelling perspective as well as in geochemical records. Here, we use a combined geochemical and modelling approach to investigate the impact of AMOC changes on surface and subsurface temperature variations in the eastern tropical North Atlantic on multi-millennial time scales and assess the potential of this temperature difference for reconstructing past AMOC variability.

* Corresponding author. Tel.: +31 614856006.

E-mail address: Raquel.Santos@nioz.nl (R.A. Lopes dos Santos).

¹ Now at California Institute of Technology Pasadena, CA 91125, United States.

2. Study location and regional setting

The geochemical records were derived from marine sediment core GeoB9528-3 (09°09.96'N, 17°39.81'W; 3057 m water depth; Fig. 1) retrieved from the Guinea Plateau Margin which spans the last 192 kyr (thousand years) (Castañeda et al., 2009). The oceanographic system of the Guinea coast region (NW Africa) is strongly influenced by deep water masses including the North Atlantic Deep Water (NADW) and also by several other surface and subsurface flows (Fig. 1). The main surface current that connects the tropical North Atlantic with the extratropics is the Canary Current (CC), which comes from the North Atlantic. It is characterized by cool, wide and slow water flow towards the equator throughout the year (Batteen et al., 2000; Wooster et al., 1976). On average, this current is about 500 m deep underlain by South Atlantic Central Water (SACW) and deeper by North Atlantic Central Water (NACW) (Wooster et al., 1976). The Antarctic Intermediate Water (AAIW) is found around 800 m depth with a salinity between 34.6 and 34.9 at the latitude of the study area. Below 1500 m, the North Atlantic Deep Water (NADW) is found with a salinity between 34.9 and 35 (Mulitza et al., 2006). This region is influenced by several other surface and subsurface currents including the North Equatorial Current (NEC) (Fig. 1), which is a broad westward flowing current, found around 7°N to about 20°N, mainly fed by cooler waters from the northeast Atlantic (Schott et al., 2002). The Equatorial Under Current (EUC), an eastward-flowing current characterized by relatively high temperature and salinity, transports heat and salt to the study area in subsurface layers of ~100 m depth (Peterson and Stramma, 1991). Near the southern boundary of the NEC, the North Equatorial Counter Current (NECC), an eastward flow, is sometimes present (Richardson and Walsh, 1986). The main source of the NECC is the retroflection from the upper layers (100 m) of the North Brazil Current (NBC), starting between 5° and 8°N (Bourles et al., 1999; Schott et al., 2002; Wilson et al., 1994). The NBC also contributes to the intermediate layers of the NECC/NEUC system (Wilson et al., 1994) and eventually to the Caribbean Current. The Guinea Dome is a thermal upwelling dome in the northeastern tropical Atlantic with the core located near 10°N, 22°W and linked to a cyclonic circulation composed of the NECC, NEUC, and NEC (Mazeika, 1967). Sediment core GeoB9528-3 is located outside the Guinea Dome (Fig. 1).

3. Materials and methods

3.1. Geochemical analyses of core GeoB9528-3

Sediment core GeoB9528-3 was sampled at 5-cm intervals for organic geochemical analyses. The age model of this core is based on

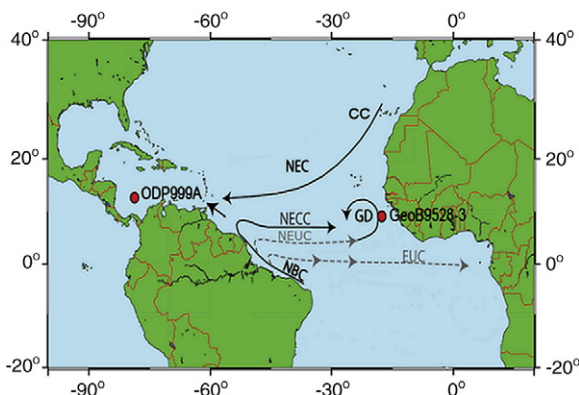


Fig. 1. Location of core GeoB9528-3 in Northwest Africa and core ODP999A (Schmidt et al., 2006) in the Cariaco basin. The black arrows indicate the major surface ocean currents in this area and the dashed arrows the main subsurface currents. CC—Canary Current, NEC—North Equatorial Current, NECC—North Equatorial Counter Current, GD—Guinea Dome, NEUC—North Equatorial Under Current, EUC—Equatorial Under Current, NBC—North Brazil Current. Figure based on Schott et al. (2004).

oxygen isotope stratigraphy of *Cibicidoides wuellerstorfi* and covers the interval from ~7 to 192 kyr. The age model has been previously published by Castañeda et al. (2009). The $\delta^{13}\text{C}$ measurements of *C. wuellerstorfi* of this core is also described by Castañeda et al. (2009) and is used as a proxy for changes in deep water circulation.

Sediment samples from the core were freeze-dried, homogenized and extracted as described by Castañeda et al. (2009). After extraction, each sample was separated into an apolar, ketone and polar fraction via alumina column chromatography using solvent mixtures of 9:1 (v/v) hexane:DCM, 1:1 hexane:DCM, and 1:1 DCM:MeOH, respectively. The alkenones were analysed for U_{37}^{K} as described previously (Castañeda et al., 2009). The polar fractions were analyzed using high-pressure liquid chromatography (HPLC). The conditions for TEX_{86} analysis of the sediments from GeoB9528-3 were described by Schouten et al. (2007). Since the location is in a tropical area, we used the $\text{TEX}_{86}^{\text{H}}$ proxy, which is applicable in high-temperature settings (>15 °C), and converted it into temperature values using the calibration of Kim et al. (2010):

$$\text{TEX}_{86}^{\text{H}} = \log \left(\frac{[\text{GDGT}-2] + [\text{GDGT}-3] + [\text{Cren}']}{[\text{GDGT}-1] + [\text{GDGT}-2] + [\text{GDGT}-3] + [\text{Cren}']} \right)$$

$$\text{Temp} [^{\circ}\text{C}] = 68.4 (\text{TEX}_{86}^{\text{H}}) + 38.6$$

3.2. NW Africa surface sediment analysis

In addition to sediment core GeoB9528-3, we also examined 12 surface sediment samples collected from NW Africa near the core location (Table 1) to obtain information on the modern distribution of U_{37}^{K} and $\text{TEX}_{86}^{\text{H}}$ ratios. The $\text{TEX}_{86}^{\text{H}}$ temperatures from these surface sediments were derived from Kim et al. (2010). The U_{37}^{K} analysis of the NW Africa surface sediment samples were done as described in Niedermeyer et al. (2009) and converted into temperature using the calibration of Müller et al. (1998).

3.3. Model experiment

To establish the equilibrated SST and subsurface temperature response in the tropical Atlantic to an AMOC shutdown, simulations were performed with the coupled atmosphere-ocean model ECBILT-CLIO. For our sensitivity experiments, we used the global atmosphere-ocean model ECBILT-CLIO version 3 (www.knmi.nl/onderzk/CKO/ecbilt.html). The coupled model derives from the atmosphere model ECBILT (Opsteegh et al., 1998) and the ocean/sea-ice model CLIO (Goosse and Fichefet, 1999). The atmospheric component solves the quasigeostrophic equations and ageostrophic correction terms in T21-resolution using three layers. The ocean component is a state-of-the-art free-surface primitive equation general circulation model which includes

Table 1

Summary table of core names locations and reconstructed temperature data from NW Africa surface sediments.

Sample (GeoB)	Latitude [°N]	Longitude [°W]	U_{37}^{K} [°C]	$\text{TEX}_{86}^{\text{H}}$ [°C]
9501	16°50.38	16°43.92	22.9	21.2
9506	15°36.48	18°20.48	24.0	23.2
9508	15°29.89	17°56.44	24.1	22.9
9510	15°24.98	17°39.24	23.7	22.2
9512	15°20.22	17°22.01	23.8	22.8
9520	13°49.76	17°35.45	23.1	22.4
9521	13°50.90	17°29.42	23.6	22.8
9525	12°38.39	17°52.76	24.6	22.7
9528	09°10.02	17°39.79	26.9	23.7
9529	09°21.19	17°22.13	27.0	23.7
9534	08°54.03	14°56.15	26.6	24.1
9535	08°52.53	14°57.62	26.8	24.0

parameterization for downsloping currents, eddy-flux parameterization for sub-gridscale horizontal mixing (Goosse et al., 1999), and a vertical mixing scheme based on the Mellor–Yamada (Mellor and Yamada, 1982) level 2.5 model (Goosse et al., 1999). These sophisticated parameterizations are of utmost importance for the simulation of the tropical thermocline which would largely be eroded by simplistic mixing with too high diffusivity. The ocean grid has a horizontal resolution of 3 degrees and 20 levels in the vertical (6 levels within the topmost 100 m). Sea-ice dynamics involves a viscous-plastic rheology. There is no local flux correction in ECBILT-CLIO. However, precipitation over the Atlantic and Arctic basins is artificially reduced by 8.5% and 25%, respectively, and homogeneously redistributed over the North Pacific. The implementation of this regional flux adjustment considerably improves the simulation of the modern climate and produces a realistic AMOC (e.g. Prange and Schulz, 2004).

From a 5000-year control run with modern boundary conditions (Prange and Schulz, 2004), three freshwater hosing experiments (with different magnitudes of globally uncompensated freshwater forcing to the North Atlantic between 50°N and 70°N: 0.1 Sv, 0.2 Sv, 0.5 Sv) were branched off. The hosing experiments were designed to elucidate the relationship between AMOC and the tropical thermocline. Freshwater hosing is a convenient and common method to slow down the AMOC in numerical climate models (e.g. Stouffer et al., 2006). We do not imply, however, that anomalous North Atlantic freshwater fluxes were the only possible forcing mechanism of Late Quaternary AMOC variations in reality. All hosing experiments were integrated for another 500 years, i.e. long enough for the AMOC and the tropical thermocline to equilibrate (Fig. 2). The last 100 years of each experiment were used for further analysis.

In order to quantify a relationship between AMOC strength (i.e. volume flux of NADW) and surface–subsurface temperature difference ΔT , we use the following approach: a considerable portion of the meridional overturning in the North Atlantic immediately recirculates north of 20°N (see Figure 1 in Prange and Schulz (2004)) and, hence,

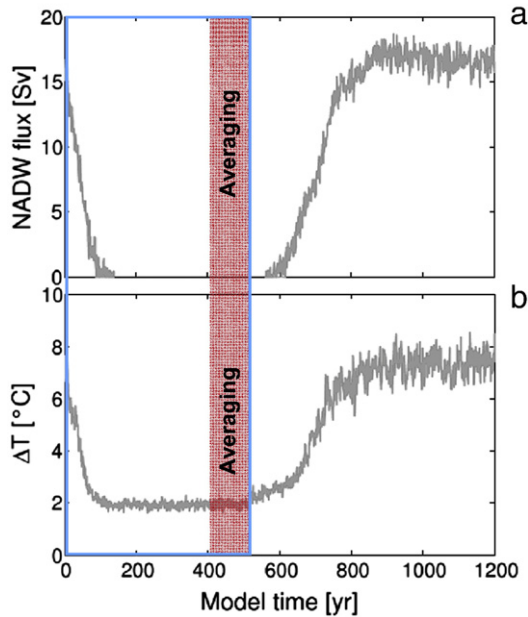


Fig. 2. Timeseries from the 0.5-Sv freshwater-hosing experiment as an example of experimental design and analysis. a, NADW volume flux (i.e. AMOC strength) calculated as described in the text. b, Surface–subsurface temperature difference ΔT , where the subsurface temperature is taken at 100 m as described in Section 4.3. Time 0 corresponds to the end of a 5000-year control run with modern boundary conditions and marks the beginning of the freshwater-hosing experiment. Freshwater was injected into the North Atlantic for 500 years (blue box). Averages from the last 100 years (red bar) were taken to construct the graph in Fig. 7.

does not contribute to the southward flow of NADW in the tropical and South Atlantic. Therefore, a better measure of NADW volume flux – which is also commonly used and which we have taken in this study – is the maximum of the meridional overturning streamfunction in the South Atlantic at 30°S (also referred to as the net export of NADW). Note that negative values are associated with the southern overturning cell and are not related to the NADW flux; therefore, negative values were set to zero.

4. Results and discussion

4.1. U_{37}^K and TEX_{86}^H temperature reconstructions in the eastern tropical North Atlantic

Two organic geochemical proxies, U_{37}^K and TEX_{86}^H , were applied to reconstruct water temperatures of the eastern tropical North Atlantic. Both the U_{37}^K index, based on the ratio of di- and tri-unsaturated long-chain ketones produced by haptophyte algae (Prahl and Wakeham, 1987), and the initial TEX_{86}^H proxy (Schouten et al., 2002), which is based on glycerol dialkyl glycerol tetraethers (GDGTs) produced by Marine Group 1 Crenarchaeota, are usually thought to reflect SST (Kim et al., 2008; Schouten et al., 2002). To confirm this, we analyzed surface sediments collected on a transect along the NW African coast (Table 1) for U_{37}^K and compared this with TEX_{86}^H values (Kim et al., 2010) for the same set of samples. This showed that the U_{37}^K index corresponds well to annual mean SST (Locarnini et al., 2006) (Fig. 3). However, TEX_{86}^H temperatures are substantially lower compared to U_{37}^K -based SST, and are similar or slightly lower than thermocline temperatures from around 30 m depth (Fig. 3). The difference between U_{37}^K and TEX_{86}^H for a number of sites is around 1.5 °C, which may be explained by the calibration errors of the two proxies (Kim et al., 2008, 2010; Müller and Fischer, 2001). However, for sites closer to the equator (<10°N) this difference is larger and up to ~3 °C (Table 1 and Fig. 3). There could be several explanations for these cooler TEX_{86}^H temperatures in comparison to the U_{37}^K . First, the TEX_{86}^H record could be influenced by input from soil-derived isoprenoid GDGTs (Weijers et al., 2006). The branched and

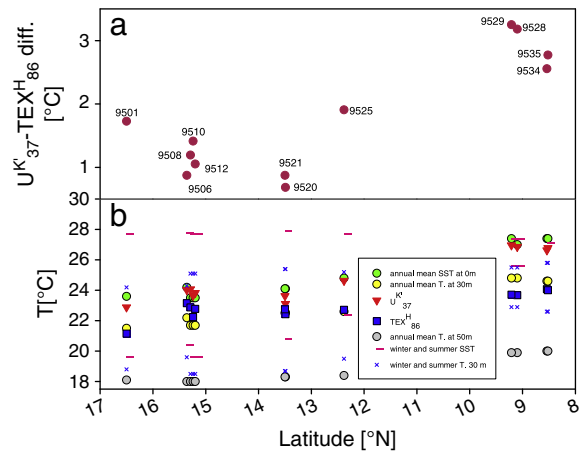


Fig. 3. U_{37}^K -derived SST, TEX_{86}^H -derived temperatures and ΔT ($U_{37}^K - TEX_{86}^H$) differences in surface sediment samples from the northwest African margin at different latitudes. a) The $U_{37}^K - TEX_{86}^H$ temperature difference plotted against latitude. The GeoB station numbers are listed next to the data points and GeoB station locations are listed in Table 1. Note that the surface sediment samples collected from latitudes of 8–10°N, including site GeoB9528–3, display the greatest difference between the U_{37}^K and TEX_{86}^H records. b) Comparison of winter, summer and annual mean SST at 0 m (Locarnini et al., 2006) and water column temperatures at 30 and 50 m (Locarnini et al., 2006) with U_{37}^K and TEX_{86}^H (Kim et al., 2010) reconstructed temperatures for GeoB stations plotted against latitude. Note that U_{37}^K derived temperatures (red triangles) agree well with SST (green circles). In contrast, TEX_{86}^H -derived temperatures (blue squares) indicate cooler temperatures compared to SST and display a better agreement with water column temperatures at 30 m (yellow circles).

isoprenoid tetraether (BIT) index (Hopmans et al., 2004) provides a method to assess the relative amount of soil organic matter input and thus possible influences on the $\text{TEX}_{86}^{\text{H}}$ record (Hopmans et al., 2004). In general, $\text{TEX}_{86}^{\text{H}}$ is considered to be applicable in settings where the BIT index is $\sim < 0.3$ (Weijers et al., 2006). However, BIT values in the surface sediments were always < 0.1 (Kim et al., 2008). These low BIT values were expected since the coring site is remote from the coast and river inputs. Thus, soil-derived GDGTs can be ruled out as an influence on the $\text{TEX}_{86}^{\text{H}}$ in this region. A second explanation for the difference in temperature values between the $\text{TEX}_{86}^{\text{H}}$ and U_{37}^{K} proxies could be due

to differences in the growth season between the source organisms (Huguet et al., 2006). Indeed, there are large seasonal variations in SST at the sites $> 10^\circ\text{N}$ but at latitudes below 10°N , including our core site GeoB9528-3, seasonal variation alone cannot explain the full temperature difference between the two proxies (Fig. 3). A third explanation could be lateral transport of GDGTs from colder areas to the region of NW Africa. However, alkenones have been shown to be affected more by long-distance lateral transport than crenarchaeol (Mollenhauer et al., 2005, 2007; Shah et al., 2008). The fact that the U_{37}^{K} values in the surface sediments correspond well to SST argues against a substantial effect of

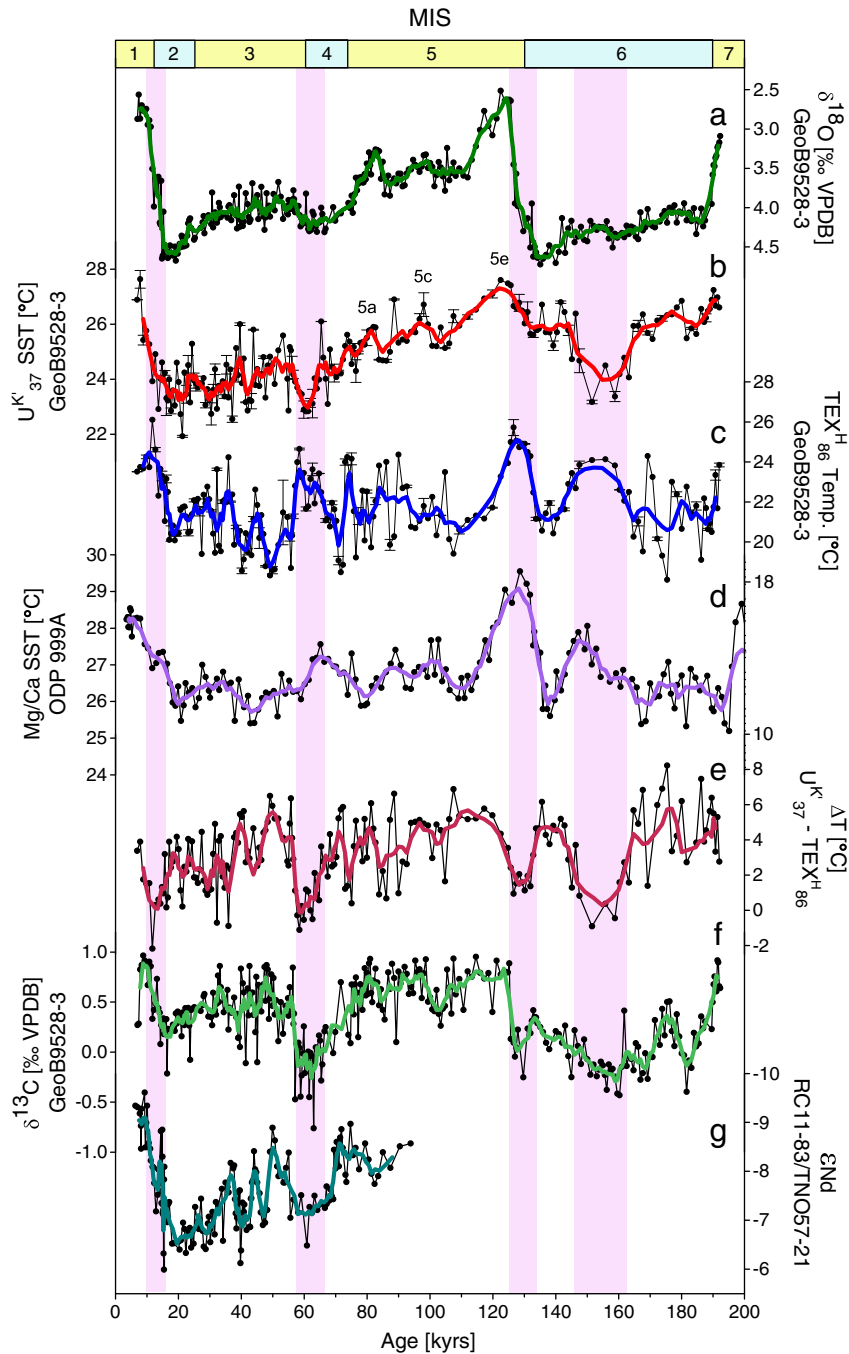


Fig. 4. Comparison of geochemical records from eastern and western tropical Atlantic. a, $\delta^{18}\text{O}$ of *C. wuellerstorfi* of eastern Atlantic core GeoB9528-3 (Castañeda et al., 2009); b, U_{37}^{K} (Castañeda et al., 2009) and c, $\text{TEX}_{86}^{\text{H}}$ records of core GeoB9528-3; the error bars on the U_{37}^{K} and $\text{TEX}_{86}^{\text{H}}$ records represent the standard deviation of multiple runs; d, Mg/Ca record from core ODP 999A from western Atlantic (Schmidt et al., 2006); e, Difference of U_{37}^{K} and $\text{TEX}_{86}^{\text{H}}$ -derived temperatures (ΔT) for GeoB9528-3; f, $\delta^{13}\text{C}$ of *C. wuellerstorfi* of core GeoB9528-3 (Castañeda et al., 2009) and g, Nd isotope ratios of core RC11-83/TNO57-21 from south Atlantic (Piotrowski et al., 2005). Shaded bars indicate periods of minor thermal stratification ($\Delta T < 2^\circ\text{C}$). The records show that depleted benthic $\delta^{13}\text{C}$ values (f) and increased neodymium isotope ratios (g), indicating that low AMOC strength, correspond to reduced ΔT (e). In all panels, the bold colored line represents the smoothed data points obtained by using a 5-point running mean whereas the black circles represent all available data points.

lateral transport in this area. Variations in upwelling intensity could be another factor influencing TEX_{86}^H temperatures as suggested by previous studies (Kim et al., 2008; Wuchter et al., 2006). However, the pattern of cooler TEX_{86}^H temperatures in comparison to U_{37}^K is observed in surface sediments located near the permanent upwelling cell of NW Africa, which is centered at ~20–25°N, but we also observe this pattern at sites located outside of the upwelling cell. Therefore, it seems that at site GeoB9528-3, upwelling is not the main cause of this temperature difference. The fifth and, in our view, the most likely explanation to explain the cooler TEX_{86}^H temperatures compared to U_{37}^K , is that TEX_{86}^H reflects a deeper and cooler water mass in comparison to the U_{37}^K index. Indeed, Crenarchaeota can reside deeper in the water column (Karner et al., 2001) and, thus, can potentially reflect temperatures of deeper water masses (Huguet et al., 2007) compared to haptophyte algae, which must remain within the photic zone. Previous studies have shown that TEX_{86} reflects subsurface rather than surface temperatures in the Santa Barbara Basin (Huguet et al., 2007) and, importantly, in the nearby Benguela upwelling region (Lee et al., 2008). In the latter study, it was found that TEX_{86} in suspended particulate matter was fairly uniform in the upper water layer and similar to TEX_{86} values in the surface sediments. TEX_{86} temperatures were substantially lower than SST, indicating a predominant contribution of crenarchaeota living in colder deeper waters. This deeper depth production may be to avoid competition for e.g., ammonia (Martens-Habbena et al., 2009). Future seasonal studies of Crenarchaeota abundance and crenarchaeotal lipid fluxes will be fundamental to better understand the TEX_{86} . However, it is reasonable to assume that in the eastern tropical Atlantic, TEX_{86}^H is reflecting subsurface temperatures, likely around the thermocline, rather than annual mean surface temperatures.

4.2. Millennial scale temperature records from the eastern tropical North Atlantic

The pattern of cooler TEX_{86}^H temperature estimates compared to U_{37}^K is also consistently found for the sedimentary record of GeoB9528-3 (Fig. 4). The difference between the two proxies is up to 7 °C, for certain time intervals, which is much larger than the present seasonal temperature variations. Thus, it seems unlikely that seasonality is the main factor leading to this temperature difference at this latitude. Since BIT values are always below 0.3 (Fig. 5), soil organic matter input has not influenced the TEX_{86}^H record. This suggests that TEX_{86}^H records subsurface temperatures over the last ~192 kyr at this site. The U_{37}^K SST corresponds well to the general trends observed in the $\delta^{18}O$ record of the benthic foraminifera *C. wuellerstorfi* (Castañeda et al., 2009) (Fig. 4a,b), displaying the warmest temperatures during interglacials, Marine Isotope Stages (MIS) 1 and 5e, and the coolest temperatures during MIS 2, 4 and 6. Previous studies noted similarities in SST between these two interglacial periods in the equatorial eastern Atlantic (Hippler et al., 2006; Weldeab et al., 2007) with the coolest SSTs during MIS 2 and MIS 6 (Weldeab et al., 2007). Interestingly, during these cold intervals, the TEX_{86}^H record registers warm conditions in the thermocline (Fig. 4b, c). Enhanced subsurface temperatures are especially pronounced during the transitions from MIS 6 to 5, 4 to 3, and 2 to 1, as well as during MIS 6 (shaded bars, Fig. 4). The transitions were paralleled by sea-level rise and presumably meltwater input into the North Atlantic, originating from a decaying Laurentide ice sheet (Carlson et al., 2007; Chang et al., 2008; Hippler et al., 2006; Piotrowski et al., 2005, 2008). An exception is the subsurface warming during MIS 6, for which there is no evidence for large-scale sea-level rise and associated meltwater injection into the North Atlantic. When comparing the $\delta^{13}C$ of *C. wuellerstorfi* from GeoB9528-3 (Castañeda et al., 2009) and a neodymium isotope (ϵ_{Nd}) record (Piotrowski et al., 2008) from the South Atlantic, both proxies for deep-water ventilation (Lynch-Stieglitz et al., 2007), we find that depleted $\delta^{13}C$ values and increased ϵ_{Nd} , indicating low AMOC strength, correspond to smaller temperature differences (ΔT) between U_{37}^K and

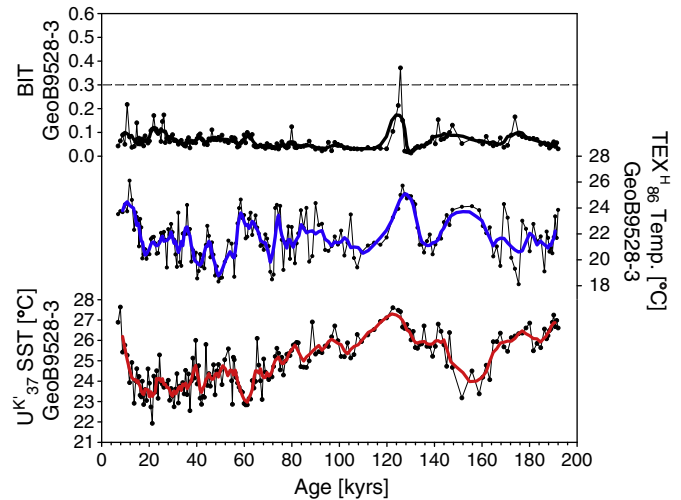


Fig. 5. BIT index values of core GeoB9528-3 (in black) together with the TEX_{86}^H (in blue) and U_{37}^K (in red) records of the same core. The dashed line represents a BIT value of 0.3. Nearly all samples in GeoB9528-3 have a BIT value of <0.3 and thus soil organic matter input is not biasing the TEX_{86}^H record.

TEX_{86}^H (Fig. 4e, f, g) thus reflecting thermocline warming during these periods.

Remarkably, there is also a significant correspondence (linear regression $r^2=0.54$; $p<0.001$) between the TEX_{86}^H temperature record and the Mg/Ca SST record from ODP site 999A from the Caribbean basin on the western side of the tropical Atlantic (Schmidt et al., 2006)

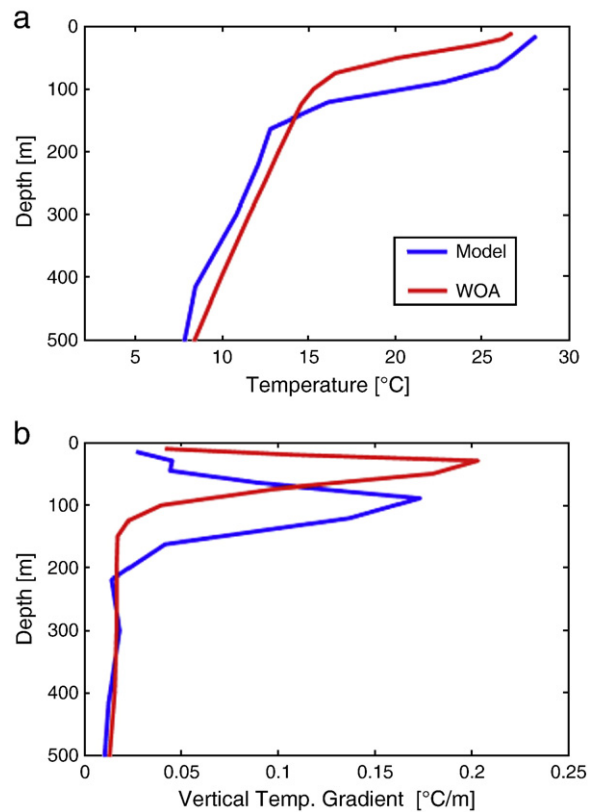


Fig. 6. Upper-ocean temperature stratification in the northeast tropical Atlantic at core location GeoB9528-3. a, profiles of annual-mean temperature in observed climatology (red) and ECBILT-CLIO modern control run (blue; calculated from long-term mean). b, corresponding vertical gradients. Data source: Locarnini et al. (2006).

(Fig. 4c,d). This is in agreement with the study of Schmidt et al. (2004), showing that during periods of AMOC slowdown, widespread surface cooling in the tropical North Atlantic is not reflected in the western Caribbean. Instead, SST warming occurs here due to the accumulation of warm and saline water in response to AMOC slowdown. This all suggests that AMOC is an important driver of the tropical thermocline adjustment processes.

4.3. Modelling tropical thermocline adjustment

Further support for the interpretation of the geochemical records comes with our modelling experiment to simulate the impact of AMOC slowdown on surface and thermocline temperatures in the eastern tropical Atlantic. The GeoB9528-3 core top data suggest that $\text{TEX}_{86}^{\text{H}}$ reflects temperatures at around 30 m depth (Fig. 3), which is close to the present day maximum vertical temperature gradient (Fig. 6). Consequently, water temperature at this depth is particularly sensitive to vertical movements of the tropical thermocline, resulting in large variations of $\text{TEX}_{86}^{\text{H}}$ temperatures in response to AMOC-induced thermocline shifts. To capture this $\text{TEX}_{86}^{\text{H}}$ signal by the climate model and hence to allow for a reasonable data-model comparison, we “measure” temperature changes at a depth close to the modelled (rather than the observed) maximum vertical temperature gradient. As shown in Fig. 6, the modelled tropical thermocline at the location of core GeoB9528-3 occurs somewhat deeper than in reality (the maximum vertical temperature gradient is at a depth of ~100 m in the model). In order to make modelled subsurface temperature variations comparable

to the $\text{TEX}_{86}^{\text{H}}$ reconstruction, we therefore use the ocean-model temperature at 100 m to calculate changes of the surface–subsurface temperature difference (ΔT) in the freshwater-hosing experiments (cf. Fig. 7c).

In a first hosing experiment with 0.5 Sv freshwater forcing, NADW formation completely stops (Fig. 2). An overall surface cooling, in comparison to modern SST, of the tropical North Atlantic is simulated, except for the western Caribbean, where SST slightly (~0.2 °C; statistically significant at the 0.01 significance level) increases (Fig. 7a). The cooling takes place only in a thin layer; below ~30 m (eastern tropical North Atlantic) to 100 m (western equatorial Atlantic) the ocean warms. Maximum warming indeed occurs around the depth of the tropical thermocline, pointing to an important role of vertical shifts in the position of the thermocline in subsurface warming. This subsurface warming leads to a substantially reduced surface–subsurface temperature difference in comparison to the control case, particularly in the eastern tropical Atlantic (Fig. 7b). These model results are thus in agreement with our $\text{TEX}_{86}^{\text{H}}$ record showing eastern tropical Atlantic subsurface warming in phase with Caribbean SST warming and AMOC slowdown.

Further model experiments with moderate AMOC slowdowns reveal that the magnitude of the surface–subsurface temperature difference at site GeoB9528-3 (Fig. 7b) scales nearly linearly with the magnitude of the AMOC anomaly (Fig. 7c). In the tropical North Atlantic, the thermocline adjustments can be ascribed to the mechanisms described above (Chiang et al., 2008; Haarsma et al., 2008; Zhang, 2007). While weakened southeast trades during times of reduced AMOC may

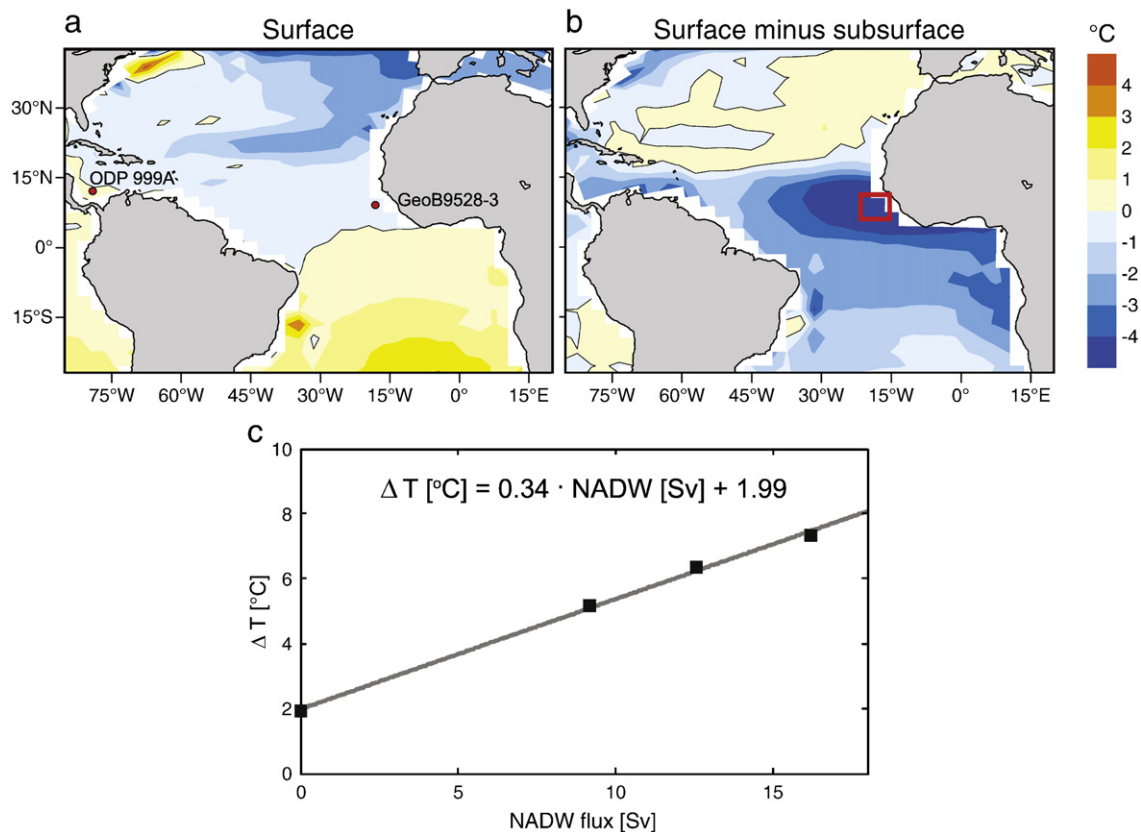


Fig. 7. Oceanic temperature response to AMOC changes simulated using a coupled climate model. a, SST difference between control run with 16.2 Sv (1 Sv = 106 m³ s⁻¹) of North Atlantic Deepwater (NADW) export (modern conditions) and a run with deepwater formation completely shut down by a strong freshwater injection into the subpolar North Atlantic. The positions of sediment cores ODP Site 999A and GeoB9528-3 are marked by red dots. b, Same as in (a) but for the surface–subsurface temperature difference anomaly, where the subsurface temperature is calculated as a vertical average over 30–200 m depth. c, relationship between absolute surface–subsurface temperature difference in the tropical northeast Atlantic around site GeoB9528-3 (area averaged over the red square indicated in b) and NADW flux, where the subsurface temperature is taken at 100 m (i.e. at the depth of the maximum vertical temperature gradient in the model as described in Section 4.3). NADW flux is defined as the maximum of the meridional overturning streamfunction in the South Atlantic at 30°S (see Section 3.3 for details). Different NADW fluxes have been obtained by varyingly strong freshwater injections. All results correspond to 100-year-averaged equilibrated annual means.

contribute to thermocline deepening in the eastern tropical South Atlantic (McIntyre and Molino, 1996), northeasterly wind anomalies over the eastern tropical North Atlantic would counteract tropical thermocline deepening here and, hence, can be ruled out as a possible driver for the observed thermocline adjustment. Our model results suggest that reconstructed surface–subsurface temperature differences may be taken as a measure of AMOC variability also on time scales much longer than decadal, and that ideal locations for reconstructing surface–subsurface temperature differences may be found in the eastern tropical North Atlantic (Fig. 7b).

Our simulations allow for a rough estimate of the AMOC variability associated with these temperature variations (Fig. 7c), although the exact number is uncertain due to uncertainties in the temperature proxies and model details and changing boundary conditions including greenhouse gases, orbital parameters and glacial ice sheets (which may influence thermocline depth through mechanisms other than AMOC changes (Paul and Schafer-Neth, 2003), but are not considered here). Using the geochemical records and the modeled relation between ΔT and NADW flux (Fig. 7c), we estimate that (multi-)millennial AMOC changes were roughly on the order of 10 Sv. While this absolute number should be interpreted carefully, it does suggest that the AMOC changes were quite substantial. These variations in tropical thermocline depth, in turn, are likely to have a substantial impact on biological productivity in the euphotic zone (McIntyre and Molino, 1996) and interannual tropical Atlantic climate variability (Haarsma et al., 2008). However, care has to be taken in interpreting this quantitative estimate as both the model and record of temperature differences across the thermocline are subject to the aforementioned uncertainties.

5. Conclusions

In the northeastern tropical Atlantic, TEX_{86}^H turns out to be a proxy for subsurface temperature. In combination with a surface paleothermometer like U_{37}^K , this allows for reconstructing past changes in tropical thermocline structure. Our sediment records and model results support the notion that a slowdown of the AMOC results in a deepening of the tropical Atlantic thermocline and that this also holds on (multi-)millennial and glacial–interglacial time scales. The depth-adjustment of the thermocline results in a change in the temperature difference between surface and subsurface. The model experiments suggest that the reconstructed temperature changes of up to 7 °C may be indicative of AMOC variations on the order of 10 Sv. Accordingly, the eastern tropical North Atlantic appears to be a particularly sensitive region for thermocline adjustments caused by the variability in AMOC strength. Sediment records from this area may thus be particularly useful for constraining past AMOC variability and its impact on the tropical Atlantic Ocean.

Acknowledgments

We thank two anonymous reviewers and editor P. Delaney for comments which improved the manuscript. We thank Marianne Baas, Ellen Hopmans, Jort Ossebaar and Michiel Kienhuis for analytical assistance with the organic geochemical analyses, and Monika Segl for assistance with the foraminiferal isotope analyses. Research funding was provided by NEBROC-2 and a VICI grant to SS from the Netherlands Organization of Scientific Research. ES, MP, SM, MS and EMN have been funded through the DFG-Research Center/Excellence Cluster “The Ocean in the Earth System”. Samples from GeoB9528-3 were supplied through the assistance of MARUM at the University of Bremen.

Appendix A. TEX_{86}^H and BIT Index data for core GeoB9528-3

Note that for one sample it was not possible to calculate a BIT value as some of the GDGTs needed to calculate this index were not present.

Appendix B. Supplementary data

Supplementary data to this article can be found online at doi:10.1016/j.epsl.2010.10.030.

References

- Batteen, M.L., Martinez, J.R., Bryan, D.W., Buch, E.J., 2000. A modeling study of the coastal eastern boundary current system off Iberia and Morocco. *J. Geophys. Res. Oceans* 105, 14173–14195.
- Bourles, B., Molinari, R.L., Johns, E., Wilson, W.D., Leaman, K.D., 1999. Upper layer currents in the western tropical North Atlantic (1989–1991). *J. Geophys. Res. Oceans* 104, 1361–1375.
- Carlson, A.E., Clark, P.U., Haley, B.A., Klinkhammer, G.P., Simmons, K., Brook, E.J., Meissner, K.J., 2007. Geochemical proxies of North American freshwater routing during the Younger Dryas cold event. *Proc. Natl. Acad. Sci. USA* 104, 6556–6561.
- Castañeda, I.S., Mulitza, S., Schefuß, E., Lopes dos Santos, R.A., Sinninghe Damsté, J.S., Schouten, S., 2009. Wet phases in the Sahara/Sahel region and human migration patterns in North Africa. *Proc. Natl. Acad. Sci. USA* 106, 20159–20163.
- Chang, P., Zhang, R., Hazeleger, W., Wen, C., Wan, X.Q., Ji, L., Haarsma, R.J., Breugem, W.P., Seidel, H., 2008. Oceanic link between abrupt changes in the North Atlantic Ocean and the African monsoon. *Nat. Geosci.* 1, 444–448.
- Chiang, J.C.H., Cheng, W., Bitz, C.M., 2008. Fast teleconnections to the tropical Atlantic sector from Atlantic thermohaline adjustment. *Geophys. Res. Lett.* 35 L07704-1–L07704-5.
- Ganachaud, A., Wunsch, C., 2003. Large-scale ocean heat and freshwater transports during the World Ocean Circulation Experiment. *J. Climate* 16, 696–705.
- Goosse, H., Fichefet, T., 1999. Importance of ice–ocean interactions for the global ocean circulation: a model study. *J. Geophys. Res. Oceans* 104, 23337–23355.
- Goosse, H., Deleersnijder, E., Fichefet, T., England, M.H., 1999. Sensitivity of a global coupled ocean–sea ice model to the parameterization of vertical mixing. *J. Geophys. Res. Oceans* 104, 13681–13695.
- Gregory, J.M., Dixon, K.W., Stouffer, R.J., Weaver, A.J., Driesschaert, E., Eby, M., Fichefet, T., Hasumi, H., Hu, A., Jungclaus, J.H., Kamenkovich, I.V., Levermann, A., Montoya, M., Murakami, S., Nawrath, S., Oka, A., Sokolov, A.P., Thorpe, R.B., 2005. A model intercomparison of changes in the Atlantic thermohaline circulation in response to increasing atmospheric CO₂ concentration. *Geophys. Res. Lett.* 32.
- Haarsma, R.J., Campos, E., Hazeleger, W., Severijns, C., 2008. Influence of the meridional overturning circulation on tropical Atlantic climate and variability. *J. Climate* 21, 1403–1416.
- Hippeler, D., Eisenhauer, A., Nägler, T.F., 2006. Tropical Atlantic SST history inferred from Ca isotope thermometry over the last 140 ka. *Geochim. Cosmochim. Acta* 70, 90–100.
- Hopmans, E.C., Weijers, J.W.H., Schefuß, E., Herfort, L., Sinninghe Damsté, J.S., Schouten, S., 2004. A novel proxy for terrestrial organic matter in sediments based on branched and isoprenoid tetraether lipids. *Earth Planet. Sci. Lett.* 224, 107–116.
- Huang, R.X., Cane, M.A., Naik, N., Goodman, P., 2000. Global adjustment of the thermocline in response to deepwater formation. *Geophys. Res. Lett.* 27, 759–762.
- Huguet, C., Kim, J.-H., Sinninghe Damsté, J.S., Schouten, S., 2006. Reconstruction of sea surface temperature variations in the Arabian Sea over the last 23 kyr using organic proxies (TEX_{86} and U_{37}^K). *Paleoceanography* 21, 1–13.
- Huguet, C., Schimmelmann, A., Thunell, R., Lourens, L.J., Sinninghe Damsté, J.S., Schouten, S., 2007. A study of the TEX_{86} paleothermometer in the water column and sediments of the Santa Barbara Basin, California. *Paleoceanography* 22 PA3203-1–PA3203-9.
- Karner, M.B., DeLong, E.F., Karl, D.M., 2001. Archaeal dominance in the mesopelagic zone of the Pacific Ocean. *Nature* 409, 507–510.
- Kim, J.-H., Schouten, S., Hopmans, E.C., Donner, B., Sinninghe Damsté, J.S., 2008. Global sediment core-top calibration of the TEX_{86} paleothermometer in the ocean. *Geochim. Cosmochim. Acta* 72, 1154–1173.
- Kim, J.-H., Meer, J.V.D., Schouten, S., Helmke, P., Willmott, V., Sangiorgi, F., Koc, N., Hopmans, E.C., Sinninghe Damsté, J.S., 2010. New indices and calibrations derived from the distribution of crenarchaeal isoprenoid tetraether lipids: implications for past sea surface temperature reconstructions. *Geochim. Cosmochim. Acta* 74, 4639–4654.
- Lee, K.E., Kim, J.-H., Wilke, I., Helmke, P., Schouten, S., 2008. A study of the alkenone, TEX_{86} , and planktonic foraminifera in the Benguela Upwelling System: implications for past sea surface temperature estimates. *Geochem. Geophys. Geosyst.* 9, 1–19.
- Locarnini, R.A., Mishonov, A.V., Antonov, J.I., Boyer, T.P., Garcia, H.E., 2006. *World Ocean Atlas 2005*. In: Levitus, S. (Ed.), *Temperature, Volume 1*. NOAA Atlas NESDIS 61, U.S. Government Printing Office, Washington, D.C. 182 pp.
- Lynch-Stiegitz, J., Adkins, J.F., Curry, W.B., Dokken, T., Hall, I.R., Herguera, J.C., Hirschi, J.J.M., Ivanova, E.V., Kissel, C., Marchal, O., Marchitto, T.M., McCave, I.N., McManus, J.F., Mulitza, S., Ninnemann, U., Peeters, F., Yu, E.F., Zahn, R., 2007. Atlantic meridional overturning circulation during the Last Glacial Maximum. *Science* 316, 66–69.
- Martens-Habbena, W., Berube, P.M., Urakawa, H., de la Torre, J.R., Stahl, D.A., 2009. Ammonia oxidation kinetics determine niche separation of nitrifying Archaea and Bacteria. *Nature* 461, 976–U234.
- Mazeika, P.A., 1967. Thermal domes in eastern tropical Atlantic Ocean. *Limnol. Oceanogr.* 12, 537–539.
- McIntyre, A., Molino, B., 1996. Forcing of Atlantic equatorial and subpolar millennial cycles by precession. *Science* 274, 1867–1870.
- Mellor, G.L., Yamada, T., 1982. Development of a turbulence closure-model for geophysical fluid problems. *Rev. Geophys.* 20, 851–875.

- Mollenhauer, G., Kienast, M., Lamy, F., Meggers, H., Schneider, R.R., Hayes, J.M., Eglinton, T.I., 2005. An evaluation of ^{14}C age relationships between co-occurring foraminifera, alkenones, and total organic carbon in continental margin sediments. *Paleoceanography* 20. doi:10.1029/2004PA001103 PA1016.
- Mollenhauer, G., Inthorn, M., Vogt, T., Zabel, M., Sinninghe Damsté, J.S., Eglinton, T.I., 2007. Aging of marine organic matter during cross-shelf lateral transport in the Benguela upwelling system revealed by compound-specific radiocarbon dating. *Geochem. Geophys. Geosyst.* 8, 1–16.
- Mulitza, S., Bouimmetarhan, I., Brüning, M., Freesemann, A., Gussone, N., Filipsson, H., Heil, G., Hessler, S., Jaeschke, A., Johnstone, H., Klann, M., Klein, F., Küster, K., März, C., McGregor, H., Minning, M., Müller, H., Ochsenhirt, W.-T., Paul, A., Schewe, F., Schulz, M., Steinlöchner, J., Stuur, J.-B., Tjallingii, R., v.Dobeneck, T., Wiesmaier, S., Zabel, M., Zonneveld, K., 2006. Report and preliminary results of Meteor-cruise M65/1, Dakar-Dakar, 11.06–1.07.2005. *Berichte aus dem Fachbereich Geowissenschaften der Universität Bremen* 252, 1–149.
- Müller, P.J., Fischer, G., 2001. A 4-year sediment trap record of alkenones from the filamentous upwelling region off Cape Blanc, NW Africa and a comparison with distributions in underlying sediments. *Deep Sea Res.* 1 48, 1877–1903.
- Müller, P.J., Kirst, G., Ruhland, G., von Storch, I., Rosell-Mele, A., 1998. Calibration of the alkenone paleotemperature index (U^k_{37}) based on core-tops from the eastern South Atlantic and the global ocean (60°N – 60°S). *Geochim. Cosmochim. Acta* 62, 1757–1772.
- Niedermeyer, E.M., Prange, M., Mulitza, S., Mollenhauer, G., Schefuss, E., Schulz, M., 2009. Extratropical forcing of Sahel aridity during Heinrich stadials. *Geophys. Res. Lett.* 36 L20707-1–L20707-4.
- Opsteegh, J.D., Haarsma, R.J., Selten, F.M., Kattenberg, A., 1998. ECBILT: a dynamic alternative to mixed boundary conditions in ocean models. *Tellus A Dyn. Meteorol. Oceanogr.* 50, 348–367.
- Paul, A., Schafer-Neth, C., 2003. Modeling the water masses of the Atlantic Ocean at the last glacial maximum. *Paleoceanography* 1058. doi:10.1029/2002PA000783.
- Peterson, R.G., Stramma, L., 1991. Upper-level circulation in the South Atlantic Ocean. *Prog. Oceanogr.* 26, 1–73.
- Piotrowski, A.M., Goldstein, S.L., Hemming, S.R., Fairbanks, R.G., 2005. Temporal relationships of carbon cycling and ocean circulation at glacial boundaries. *Science* 307, 1933–1938.
- Piotrowski, A.M., Goldstein, S.L., Hemming, S.R., Fairbanks, R.G., Zylberberg, D.R., 2008. Oscillating glacial northern and southern deep water formation from combined neodymium and carbon isotopes. *Earth Planet. Sci. Lett.* 272, 394–405.
- Prahl, F.G., Wakeham, S.G., 1987. Calibration of unsaturation patterns in long-chain ketone compositions for palaeotemperature assessment. *Nature* 330, 367–369.
- Prange, M., Schulz, M., 2004. A coastal upwelling seesaw in the Atlantic Ocean as a result of the closure of the Central American Seaway. *Geophys. Res. Lett.* 31, L17207. doi:10.1029/2004GL020073.
- Rahmstorf, S., 2002. Ocean circulation and climate during the past 120, 000 years. *Nature* 419, 207–214.
- Richardson, P.L., Walsh, D., 1986. Mapping climatological seasonal variations of surface currents in the tropical Atlantic using ship drifts. *J. Geophys. Res. Oceans* 91, 537–550.
- Schmidt, M.W., Spero, H.J., Lea, D.W., 2004. Links between salinity variation in the Caribbean and North Atlantic thermohaline circulation. *Nature* 428, 160–163.
- Schmidt, M.W., Vautravers, M.J., Spero, H.J., 2006. Western Caribbean sea surface temperatures during the late Quaternary. *Geochem. Geophys. Geosyst.* 7, 1–17.
- Schott, F.A., Brandt, P., Hamann, M., Fischer, R., Stramma, L., 2002. On the boundary flow off Brazil at 5 – 10°S and its connection to the interior tropical Atlantic. *Geophys. Res. Lett.* 29 1840. doi:10.1029/2002GL014786.
- Schott, F.A., McCreary, J.P., Johnson, G.C., 2002. Shallow Overturning Circulations of the Tropical-Subtropical Oceans. *Geophysical Monograph* 147, 261–304.
- Schouten, S., Hopmans, E.C., Schefuß, E., Sinninghe Damsté, J.S., 2002. Distributional variations in marine crenarchaeotal membrane lipids: a new tool for reconstructing ancient sea water temperatures? *Earth Planet. Sci. Lett.* 204, 265–274.
- Schouten, S., Forster, A., Panoto, F.E., Sinninghe Damsté, J.S., 2007. Towards calibration of the TEX₈₆ palaeothermometer for tropical sea surface temperatures in ancient greenhouse worlds. *Org. Geochem.* 38, 1537–1546.
- Shah, S.R., Mollenhauer, G., Ohkouchi, N., Eglinton, T.I., Pearson, A., 2008. Origins of archaeal tetraether lipids in sediments: insights from radiocarbon analysis. *Geochim. Cosmochim. Acta* 72, 4577–4594.
- Stouffer, R.J., Yin, J., Gregory, J.M., Dixon, K.W., Spelman, M.J., Hurlin, W., Weaver, A.J., Eby, M., Flato, G.M., Hasumi, H., Hu, A., Jungclaus, J.H., Kamenkovich, I.V., Levermann, A., Montoya, M., Murakami, S., Nawrath, S., Oka, A., Peltier, W.R., Robitaille, D.Y., Sokolov, A., Vettoretti, G., Weber, S.L., 2006. Investigating the causes of the response of the thermohaline circulation to past and future climate changes. *J. Climate* 19, 1365–1387.
- Weijers, J.W.H., Schouten, S., Spaargaren, O.C., Sinninghe Damsté, J.S., 2006. Occurrence and distribution of tetraether membrane lipids in soils: Implications for the use of the TEX₈₆ proxy and the BIT index. *Org. Geochem.* 37, 1680–1693.
- Weldeab, S., Lea, D.W., Schneider, R.R., Andersen, N., 2007. 155, 000 years of West African monsoon and ocean thermal evolution. *Science* 316, 1303–1307.
- Wilson, W.D., Johns, E., Molinari, R.L., 1994. Upper layer circulation in the western tropical North Atlantic Ocean during August 1989. *J. Geophys. Res. Oceans* 99, 22513–22523.
- Wooster, W.S., Bakun, A., McClain, D.R., 1976. The seasonal upwelling cycle along eastern boundary of North Atlantic. *J. Mar. Res.* 34, 131–141.
- Wuchter, C., Schouten, S., Wakeham, S.G., Sinninghe Damsté, J.S., 2006. Archaeal tetraether membrane lipid fluxes in the northeastern Pacific and the Arabian Sea: implications for TEX₈₆ paleothermometry. *Paleoceanography* 21 PA4208-1–PA4208-9.
- Zhang, R., 2007. Anticorrelated multidecadal variations between surface and subsurface tropical North Atlantic. *Geophys. Res. Lett.* 34 , L12713. doi:10.1029/2007GL030225.